Acid-Sensitive Polymeric Micelles Based on Thermoresponsive Block Copolymers with Pendent Cyclic Orthoester Groups

ARTICLE *in* MACROMOLECULES · JANUARY 2009

Impact Factor: 5.8 · DOI: 10.1021/ma802138r

8 AUTHORS, INCLUDING:

Fu-Sheng Du
Peking University
98 PUBLICATIONS **1,939** CITATIONS
SEE PROFILE

Jing Cheng
Northwestern University
6 PUBLICATIONS **95** CITATIONS
SEE PROFILE

Zichen Li
Peking University
161 PUBLICATIONS **3,507** CITATIONS
SEE PROFILE

Acid-Sensitive Polymeric Micelles Based on Thermoresponsive Block Copolymers with Pendent Cyclic Orthoester Groups

Xiaonan Huang,[†] Fusheng Du,*[,†] Jing Cheng,[†] Yongquan Dong,[†] Dehai Liang,*[,†] Shouping Ji,[‡] Shrong-Shi Lin,[†] and Zichen Li*[,†]

Beijing National Laboratory for Molecular Sciences, Key Laboratory of Polymer Chemistry and Physics of Ministry of Education, College of Chemistry & Molecular Engineering, Peking University, Beijing 100871, China, and Department of Molecular Biology, Beijing Institute of Transfusion Medicine, Beijing 100850, China

Received September 20, 2008; Revised Manuscript Received November 24, 2008

ABSTRACT: An orthoester-containing monomer, *trans*-*N*-(2-ethoxy-1,3-dioxan-5-yl)acrylamide (*t*NEA), was synthesized. Atom transfer radical polymerization of *t*NEA using a poly(ethylene glycol) (PEG) macroinitiator afforded three acid-labile thermoresponsive block copolymers: PEG-*b*-P*t*NEA$_{27}$, PEG-*b*-P*t*NEA$_{56}$, and PEG-*b*-P*t*NEA$_{73}$. These block copolymers are water-soluble at low temperatures (<13 °C). Thermally induced phase transition behaviors, including the critical aggregation temperatures (CATs), of these polymers were investigated by light scattering and ^{1}H NMR. The results indicated that the longer the P*t*NEA chain length, the lower the CAT. Upon heating above the CATs, all the three polymers underwent a phase transition and formed polymeric micelles or micelle-like nanoparticles with PEG as the shell and P*t*NEA block as the core. Both the sizes and morphologies of the micelles were found to be affected by the heating rate and the salt concentration in the buffers. The micelles, formed through a fast heating procedure in the buffer with a relatively high salt concentration, have a smaller size and a more compacted structure. pH-dependent destabilization of the polymeric micelles prepared from PEG-*b*-P*t*NEA$_{73}$ was studied by using light scattering and Nile Red fluorescence. The results demonstrated that hydrophobic Nile Red could be loaded in the micelles that were stable at pH 7.4, but destabilized in mildly acidic media. The dissociation of the micelles and the subsequent release of Nile Red were induced by the acid-triggered hydrolysis of the orthoester groups, which was proved by the ^{1}H NMR spectra.

Introduction

Amphiphilic block copolymers are known to self-assemble into aggregates with various supramolecular micro/nanostructures in selective solvents.[1] Among them, the polymeric micelles or micelle-like structures formed in aqueous solution by the assembly of amphiphilic block copolymers have been extensively investigated due to their great potential as drug carriers.[2] The unique characteristics, such as the mesoscopic size and the core−shell structure, make the polymeric micelles attractive candidates for the systemic delivery of hydrophobic drugs, especially those with harmful side effects. The micelles with a size range of ∼10−100 nm and a flexible, hydrophilic shell can avoid rapid glomerular excretion in the kidney and thus reduce the undesirable clearance by the reticuloendothelial system.[3] This prolongs the circulation time of the micelles in blood and promotes their passive accumulation at the pathological sites such as tumor tissues through the well-known enhanced permeation and retention (EPR) effect.[4] In addition, polymeric micelles generally possess lower critical aggregation concentration compared with those formed by the low molecular weight surfactants and show good thermodynamic as well as dynamic stability, which is beneficial when the hydrophobic drug-loaded micelles are used intravenously.[5]

For systemic applications of the drug-loaded polymeric micelles, one important issue is how to tune the drug release in a controlled fashion. It is preferred that the micelles remain stable without or with little drug leakage during the blood circulation but release the drug after reaching the target sites. To achieve this goal, various stimuli-responsive polymeric micelles or nanoparticles, including thermo-, pH-, ultrasound-, light-, redox-, and enzyme-sensitive systems, have been developed.[6,7] In particular, pH-sensitive polymeric micelles or nanoparticles as drug carriers are the most thoroughly studied since there are numerous pH gradients existing in both normal and pathological states. In general, pH-sensitive polymeric micelles can be formed by the block copolymers containing weakly basic or acidic groups.[8] Recently, Frechet and co-workers reported an alternative approach to acid-sensitive micelles by attaching hydrophobic groups to the periphery of the core-forming dendritic block through a cyclic acetal linkage.[9] The doxorubicin (DOX)-loaded micelles demonstrated a different intracellular distribution compared with the free drug and showed a promise as carriers for the triggered release of therapeutics in mildly acidic environments.[10] Kataoka et al. prepared polymeric micelles by attaching DOX to the amino acid units of a PEG-*b*-P(aspartic acid) via hydrazone linkage.[11] Also, Park and co-workers reported a block copolymer composed of PEG and poly(L-lactic acid) with terminally conjugated DOX through a hydrazone or *cis*-aconityl bond, which formed micelles. These acid-sensitive micelles had a much faster release of free DOX at pH 5 than at the neutral pH.[12]

Temperature is another commonly used stimulus for intelligent systems which have potential for biomedical and pharmaceutical applications. Thermoresponsive polymers and the relevant nanoparticles or hydrogels have been well documented in some reviews.[13] Taking poly(*N*-isopropylacrylamide) (PNIPAM) as an example, it can be introduced into polymeric micelles as a hydrophilic shell or as a hydrophobic core.[6a] Okano et al. reported the DOX-loaded polymeric micelles composed of a PLA core and a poly(NIPAM-*co*-*N*,*N*-dimethylacrylamide) shell, which had a cloud point (CP) of 40 °C. Above the CP, DOX release was much faster than at 37 °C, which was attributed to the structure distortion of the core caused by the thermally induced collapse of the shell.[14] By contrast, block copolymers of PNIPAM and other hydrophilic segments, such as PNIPAM-

* Corresponding authors. E-mail: fsdu@pku.edu.cn (F.D.); zcli@pku.edu.cn (Z.L.); dliang@pku.edu.cn (D.L.).
† Peking University.
‡ Beijing Institute of Transfusion Medicine.

10.1021/ma802138r CCC: $40.75
Published on Web 01/16/2009

Scheme 1. Thermally Induced Formation and Acid-Triggered Dissociation of the Polymeric Micelles

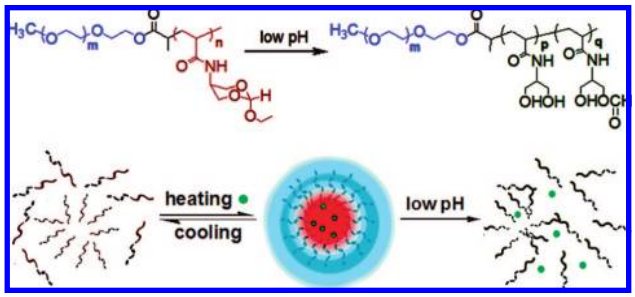

b-PEG, can self-assemble into micelles or vesicles simply by heating.[15] Hennink et al. reported novel types of polymeric micelles which were formed from hydrolyzable thermoresponsive block copolymers at the physiological temperature but gradually dissociated with hydrolysis of the pendent lactate groups. One of the unique features of these micelles is that the hydrophobic drugs such as paclitaxel can be loaded in the micelles by quickly heating above the critical micelle temperature of the block copolymers, without using any harmful organic solvents.[16] However, these micelles hydrolyzed in neutral or basic buffers but were relatively stable in mildly acidic media.

Recently, we prepared a type of acid-labile thermoresponsive poly(methacrylamide) with pendent orthoester moieties. The aggregates formed by the polymers at temperature above the CP were dissolved gradually with the hydrolysis of the orthoester groups.[17] In contrast to the hydrolyzable thermoresponsive polymers reported by other groups,[16,18] our polymers are susceptible to hydrolysis under mildly acidic environments but relatively stable in neutral or weakly basic aqueous solutions. On the basis of these results, we report a new type of acid-labile thermoresponsive block copolymers composed of a PEG block and a polyacrylamide segment with pendent cyclic orthoester groups (Scheme 1). Upon heating above their CATs, these copolymers spontaneously form polymeric micelles or micelle-like nanoparticles which can encapsulate hydrophobic molecules. In addition, these micelles or micelle-like nanoparticles are stable at neutral pH but gradually dissociate in mildly acidic environments, which would trigger the release of the payloads.

Experimental Section

Materials. 2-Amino-1,3-propanediol (Huaqingrunde Co., Beijing, China), triethyl orthoformate, D_2O, 2-chloropropionyl chloride, 4-(dimethylamino)pyridine (Acros), and poly(ethylene glycol) monomethyl ether (M_n = 5000 Da, PEG_{114}, Fluka) were used as received. Tetrahydrofuran (THF) and 2-propanol were distilled over sodium prior to use. *N*,*N*-Dimethylformamide (DMF) was dried with anhydrous K_2CO_3 overnight and distilled under reduced pressure. CuCl (99%, Acros) was washed with acetic acid and then ethyl ether. $CDCl_3$ (Acros) was treated with anhydrous K_2CO_3 for NMR measurements of the orthoester-containing samples. Acryloyl chloride was synthesized from acrylic acid and benzoyl chloride according to the literature.[19] *N*-(1,3-Dihydroxypropan-2-yl)acrylamide was synthesized by the same procedure as for its methacrylamide analogue.[17a] 2-Chloropropionate-containing PEG macroinitiator, PEG_{114}-Cl, was prepared from 2-chloropropionyl chloride and PEG_{114} according to the procedure in the literature.[20] Tris(2-dimethylaminoethyl)amine (Me_6TREN) was synthesized according to the literature's method with minor modification.[21] Other solvents and reagents were used as received.

Synthesis of tNEA. A mixture of *trans*- and *cis*-*N*-(2-ethoxy-1,3-dioxan-5-yl)acrylamide (*t*NEA and *c*NEA) was prepared following a similar procedure as reported in a previous paper.[17a] Briefly, *N*-(1,3-dihydroxypropan-2-yl)acrylamide (10 g, 0.069 mol), triethyl orthoformate (10.2 g, 0.069 mol), and *p*-toluenesulfonic acid monohydrate (0.13 g, 0.69 mmol) were dissolved in 200 mL of dried THF. The reaction mixture was stirred at ambient temperature for 2 h. After removing most part of the solvent under reduced pressure, the residue was prepurified via an Al_2O_3 column using ethyl acetate as the eluent. The yield of the crude product with a mixture of *trans* and *cis* isomers was 87%. The isomers were further isolated by repeated chromatography through an Al_2O_3 column with a mixed solvent of hexane and ethyl acetate (5:2, v/v). After crystallization from hexane/THF (5:1, v/v), a white crystal of *t*NEA was obtained in a total yield of ~25%; mp 74.4−76.5 °C. ^{1}H NMR (TMS, $CDCl_3$, 400 MHz, ppm, Figure S1): 6.52 (s, 1H, −N*H*CO−), 6.33 (d, 1H, CH_2=C*H*−), 6.15 (m, 1H, CH_2=CH−), 5.70 (d, 1H, CH_2=CH−), 5.45 (s, 1H, CHO_3), 4.40 (d, 2H, N−CH(CH_2)$_2$, axial), 4.10 (m, 1H, N−C*H*(CH_2)$_2$), 3.64 (d, 2H, N−CH(CH_2)$_2$, equatorial), 3.61 (q, 2H, −OCH_2CH$_3$), 3.61 (q, 2H, −OCH$_2$CH_3). ^{13}C NMR ($CDCl_3$, 75 MHz, ppm, Figure S1): 165.0 (−*C*=O), 130.5 (CH_2=*C*−), 127.0 (*C*H_2=C−), 107.4 (−*C*HO$_3$), 62.0 (N−CH(*C*H$_2$)$_2$), 61.5 (−O*C*H$_2$CH$_3$), 43.5 (N−*C*H(CH$_2$)$_2$), 14.8 (−OCH$_2$*C*H$_3$). FT-IR (KBr, cm^{-1}): 3256, 3061, 2976, 2949, 1654, 1618, 1548, 1071, 1033, 1009. MS: 200 $(M - 1)^+$. Elemental analysis: Calcd C% 53.72, N% 6.96, H% 7.51; Found C% 54.20, N% 6.84, H% 7.59.

ATRP of *t*NEA. Block copolymers with different P*t*NEA chain lengths, PEG-*b*-P*t*NEAs, were prepared by atom transfer radical polymerization (ATRP). Take PEG-*b*-P*t*NEA_{73} as an example. *t*NEA (0.5 g, 2.5 mmol), Me_6TREN (5.7 mg, 0.025 mmol), and PEG_{114}-Cl (0.125 g, 0.025 mmol) were charged into a polymerization tube, to which a mixture of 2-propanol (0.5 g) and DMF (0.5 g) was added to dissolve the monomer and initiator. After three cycles of freeze−pump−thaw to thoroughly remove oxygen, CuCl (2.5 mg, 0.025 mmol) was added into the tube under a nitrogen atmosphere, and the tube was sealed in vacuo. The polymerization was carried out at 40 °C for 18 h. Then, the reaction mixture was diluted with 5 mL of THF and passed through an Al_2O_3 column to remove the catalyst. The polymers were precipitated from ethyl ether thrice, collected by filtration, and dried in vacuo to afford white powder (70% yield). Other two block copolymers, PEG-*b*-P*t*NEA_{27} (69% yield) and PEG-*b*-P*t*NEA_{56} (41% yield), were prepared by a similar procedure but using different feed ratios. The obtained polymers were characterized by gel permeation chromatography (GPC) and ^{1}H NMR.

GPC Measurement. GPC measurements were carried out by using equipment composed of a Waters 1525 binary HPLC pump, a Waters 2414 refractive index detector, and three Waters Styragel columns (HT2, HT3, and HT4). The columns were placed in a thermostat at 35 °C, and THF was used as eluent with a flow rate of 1 mL/min. A series of narrow dispersed polystyrenes were used as the standards, and a Millennium 32 software was applied to calculate the molecular weight and polydispersity index.

NMR Spectroscopy. ^{1}H NMR spectra in $CDCl_3$ of the monomer and polymers including the PEG macroinitiator were recorded on a Bruker 400 spectrometer using tetramethylsilane (TMS) as the internal reference. Temperature-dependent ^{1}H NMR spectra of the block copolymers in the deuterated buffers (pD 8.4) and ^{13}C NMR spectrum in $CDCl_3$ of *t*NEA were obtained on a Varian Mercury Plus 300 NMR spectrometer.

Light Scattering Measurements. A commercial laser light scattering spectrometer (Brookhaven Inc., Holtsville, NY) equipped with a BI-200SM goniometer and a BI-TurboCorr digital correlator was used for both dynamic light scattering (DLS) and static light scattering (SLS) measurements. A 100 mW vertically polarized solid state laser (532 nm, CNI, Changchun, China) was used as the light source.[15c,17b] For DLS experiments, the intensity−intensity time correlation function $G^{(2)}(t,\theta)$ was measured in the self-beating mode, which is related to the normalized first-order electric field time correlation function $g^{(1)}(t,\theta)$ as $G^{(2)}(t,\theta) = A[1 + \beta|g^{(1)}(t,\theta)|^2]$, where A is the measured baseline, β is a spatial coherence factor, t is the delay time, and θ is the scattering angle. $g^{(1)}(t,\theta)$ is further related to the line width distribution $G(\Gamma)$. By using a Laplace

inversion program, CONTIN, the normalized distribution function $G(\Gamma)$ of the characteristic line width was obtained. The line width Γ is a function of both concentration (C) and scattering vector q, which can be expressed as $\Gamma/q^2 = D(1 + k_dC)[1 + f(R_gq)^2]$, where $q = (4\pi n/\lambda_0)\sin(\theta/2)$, with D, k_d, f, R_g, n, and λ being the translational diffusive coefficient, the diffusion second virial coefficient, a dimensionless constant, the z-averaged root-mean-square radius of gyration, the solvent refractive index, and the incident wavelength in vacuo, respectively. When the concentration is dilute and $R_gq \ll 1$, Γ/q^2 is approximately equal to D. D can be further converted into the hydrodynamic radius (R_h) by using the Stokes−Einstein equation $D = k_BT/6\pi\eta R_h$, where k_B, T, and η are the Boltzmann constant, the absolute temperature, and the viscosity of the solvent, respectively. In the present work, we extrapolated Γ/q^2 to zero angle to obtain the apparent hydrodynamic radius $R_{h,app}$. According to the SLS theory,[22] for a dilute solution detected at a relatively small scattering angle, the excess Rayleigh ratio ($R_{vv}(q)$) is related to the weight-averaged molecular weight (M_w), R_g, the second virial coefficient (A_2) as

$$KC/R_{vv}(q) \approx (1/M_w)(1 + R_g^2q^2/3) + 2A_2C \quad (1)$$

where $K = 4\pi^2n^2(dn/dc)^2/(N_A\lambda_0^4)$ with N_A and dn/dc being Avogadro's constant and the specific refractive index increment, respectively. In the present study, SLS measurements were carried out in the scattering angle range of 20°−120°. The time-averaged light scattering intensity (I_θ) can be written as $I_\theta = (I_{\theta,solution} - I_{\theta,solvent})\sin(\theta)$, where $I_{\theta,solution}$ and $I_{\theta,solvent}$ denote the scattering intensity at θ angle of the polymer solution and the solvent, respectively. $R_{vv}(q)$ can be related to I_θ as $R_{vv}(q) = R_{90,toluene}(I_\theta/I_{90,toluene})(n/n_{toluene})^2$, where $R_{90,toluene}$ is the Rayleigh ratio of toluene detected at 90°. $I_{90,toluene}$ and $n_{toluene}$ are the scattering intensity detected at 90° and the refractive index of toluene. For a dilute solution at a given polymer concentration, eq 1 can be simplified as

$$1/R_{vv}(q) \approx (1/M_wKC)(1 + R_g^2q^2/3) \quad (2)$$

$R_{g,app}$ is calculated from the intercept and slope in the plot of $1/R_{vv}(q)$ vs q^2 according to eq 2.

Thermally Induced Phase Transition. The block copolymer solutions at 1.0 mg/mL were prepared in 10 mM phosphate buffer (pH 8.4) at low temperatures. The purpose of using the pH 8.4 phosphate buffer is to avoid the potential hydrolysis of orthoester groups during the measurements. The polymer solutions were stored in a refrigerator (~4 °C) for ~24 h to ensure the complete dissolution of the polymers and dust-freed by a 0.45 μm filter prior to the light scattering measurements. During the study of the thermally induced phase transition by light scattering, two heating procedures were applied. In the slow heating procedure, the sample vial placed in a brass holder was heated 1−2 °C per step and equilibrated at each temperature for ~60 min before the measurements. The critical association temperature (CAT) was determined from the plot of light scattering intensity vs temperature. CAT was defined as the intersection of the horizontal tangent through the points at low temperatures with the line drawn through the points of the drastically increasing regions at high temperatures. In the fast heating procedure, the polymer solutions at ~4 °C were quickly heated to 60 °C within 5 min, stayed for another 10 min at this temperature, and then slowly cooled to 37 °C (~1 h).

Destabilization of Micelles Monitored by Light Scattering. The destabilization experiments of the micelles monitored by light scattering were carried out at 37 °C at two different pHs: 7.4 and 5.0. For pH 7.4, the polymer was first dissolved in 10 mM phosphate buffer (pH 8.4) with a concentration of 2.0 mg/mL at low temperature and stored in a refrigerator (~4 °C) overnight. This stock solution was diluted with an equal volume of pH 7.4 phosphate buffer (200 mM), clarified by a 0.45 μm filter, and subjected to the fast heating procedure to prepare polymeric micelles just prior to the light scattering measurements. For pH 5.0, the polymeric micelle solution (2.5 mL) with a polymer concentration of 1.0 mg/mL was first prepared by the fast heating procedure in pH 8.4 phosphate buffer (10 mM) as mentioned in the previous section. The light scattering data of this solution were taken as those for the 0 time point. After addition of ~50 μL pH 5.0 acetate buffer (5 M), the micelle solution was mixed thoroughly and the light scattering measurements were performed at the desired time points at 37 °C.

Scheme 2. Synthesis of PEG-*b*-P*t*NEA[a]

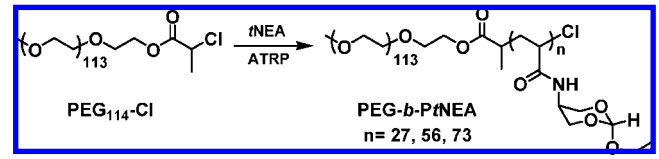

[a] ATRP conditions: CuCl, Me_6TREN, 40 °C, 18 h, in DMF/2-propanol.

Acid-Triggered Release of Nile Red. The pH-dependent release behaviors of Nile Red were studied at four different pHs. For pH 4.0 (or 5.0), 50 μL of Nile Red in ethanol (5.0×10^{-4} mol/L) was added into 5.0 mL of polymer solution (1.0 mg/mL) in 10 mM pH 8.4 phosphate buffer. After being stored in a refrigerator (~4 °C) for ~2 h, the solution was quickly heated to 37 °C and incubated overnight to equilibrate the Nile Red and the formed micelles. The emission spectrum of the micelle solution was recorded at 37 °C as for the 0 time point. After addition of 20 μL of 5 M pH 4.0 (or 5.0) acetate buffer into 1.0 mL of the micelle solution, the emission spectra of the thoroughly mixed solution were measured at the desired time points. In the case of pH 6.0 (or 7.4), a stock micelle solution (2.0 mg/mL) with Nile Red (1.0×10^{-5} mol/L) was prepared in 10 mM pH 8.4 phosphate buffer. The solution was diluted with an equal volume of 0.2 M pH 6.0 (or 7.4) phosphate buffer just prior to fluorescence detection. Then its emission spectra were measured at the desired time points. An F-4500 fluorometer (Hitachi) was used for the fluorescence measurements, with both emission and excitation slit widths being 5 nm. The emission spectra were recorded from 560 to 700 nm with an excitation wavelength of 545 nm.

Results and Discussion

Synthesis and Characterization of Monomer and Block Copolymers. Monomer *t*NEA was synthesized according to the similar procedure as that for its methacrylamide analogue, *t*NEM.[17b] The chemical structure and configuration of *t*NEA were confirmed by its ^{1}H and ^{13}C NMR spectra, mass spectrum, and single-crystal X-ray diffraction measurement (Figures S1−S3). Diblock copolymers, PEG-*b*-P*t*NEAs, were prepared by ATRP (Scheme 2). It was reported that well-defined polymers of NIPAM can be prepared by ATRP using the combination of a 2-chloropropionate-containing initiator and Me_6TREN as the ligand.[23] Thus, a PEG macroinitiator with the 2-chloropropionate at one end was used for the ATRP of *t*NEA. Although 2-propanol was reported to be a good solvent for the ATRP of NIPAM,[23a] a mixture of DMF and 2-propanol was used in the present study because the PEG macroinitiator and the obtained copolymers were not well soluble in pure 2-propanol. Three block copolymers with different lengths of P*t*NEA block were prepared by changing the feed ratio of the monomer to macroinitiator (Table 1 and Figure S5). They all had unimodal GPC traces with narrow molecular weight distributions. The degree of polymerization of P*t*NEA block was determined by comparing the peak intensities of the methoxy proton (a) at ~3.4 ppm and the orthoester proton (i) at ~5.5 ppm in the ^{1}H NMR spectrum (Figure 1).

Solution Properties below Phase Transition Temperature. All three copolymers (**P1**, **P2**, and **P3**) were water-soluble, and the polymer solutions were visually transparent below a

Table 1. ATRP Conditions and Characterization of PEG-*b*-P*t*NEA Copolymers

		[M]:[I]:[CuCl]:[L][a]	yield (%)	M_n[b] ($\times 10^4$)	PDI[b]	$M_{n,NMR}$[c] ($\times 10^4$)	CAT[d] (°C)
P1	PEG-*b*-P*t*NEA$_{27}$	30:1:1:1	69	1.15	1.13	1.04	17.5
P2	PEG-*b*-P*t*NEA$_{56}$	60:1:1:1	41	1.34	1.23	1.62	14.8
P3	PEG-*b*-P*t*NEA$_{73}$	100:1:1:1	70	1.57	1.27	1.97	13.7

[a] M, I, and L denote the monomer, macroinitiator, and Me_6TREN, respectively. [b] Number-averaged molecular weight and polydispersity index determined by GPC with THF as an eluent and monodisperse polystyrenes as the standards. [c] Number-averaged molecular weight determined by ^1H NMR. [d] Determined by light scattering.

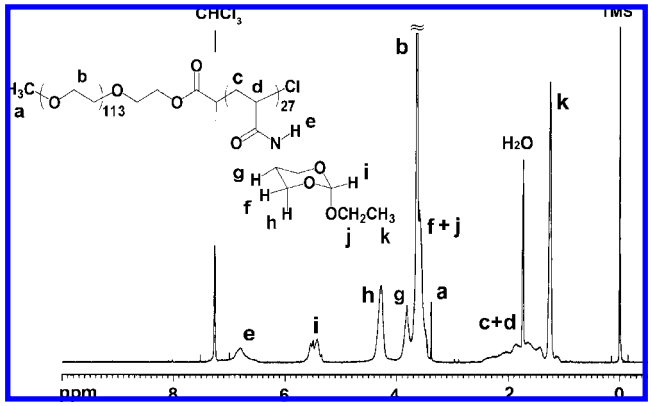

Figure 1. ^1H NMR spectrum of PEG-*b*-P*t*NEA$_{27}$ (**P1**) in $CDCl_3$.

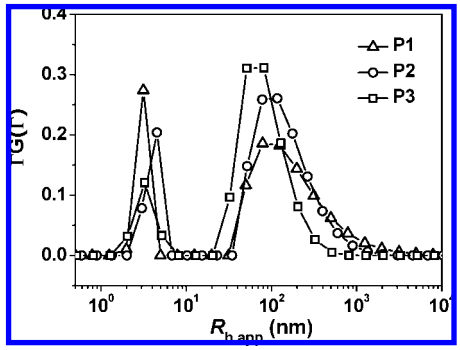

Figure 2. CONTIN analysis of PEG-*b*-P*t*NEA$_{27}$ (**P1**), PEG-*b*-P*t*NEA$_{56}$ (**P2**), and PEG-*b*- P*t*NEA$_{73}$ (**P3**) in 10 mM phosphate buffer (pH 8.4). Polymer concentration: 1.0 mg/mL; detection angle: 90°; temperature: 10 °C for **P1** and **P2** and 11 °C for **P3**.

specific temperature, i.e., the CAT. However, DLS results show a bimodal distribution for all the three copolymers at temperature below the CAT, indicating the occurrence of association (Figure 2). Besides the smaller component with an apparent hydrodynamic radius ~3 nm that can be attributed to the individual polymer chains, a much larger component belonging to the associates coexists in the system. Similar association phenomena were also observed for the block or graft copolymers of PNIPAM and PEG below the lower critical solution temperature (LCST),[15a,24] and the formed associates were reported to be in a loose and thermodynamically reversible conformation.[15c] The driving force for the association of PEG-*b*-P*t*NEA may come from the P*t*NEA block, which itself showed association behavior even below its LCST (data not shown). In addition, our previous study indicated that poly(*N*-(2-ethoxy-1,3-dioxan-5-yl)methacrylamide), a homopolymer having similar pendent groups as P*t*NEA, formed associates below its phase transition temperature.[17b]

Although the peak area of the loose associates was larger than that of the smaller component for each of the copolymers, the weight percentage of these associates was deduced to be very small. It is known that the amplitudes in $\Gamma G(\Gamma)$ from the CONTIN analysis are averaged by the scattered intensity. Since the scattered intensity is approximately proportional to the sixth power of the particle size, the number of the associates in Figure 2 was much less than that of the single polymer chains.[25,26]

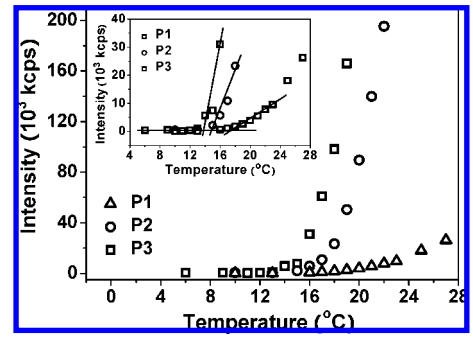

Figure 3. Temperature dependence of the excess scattered intensity of the polymer aqueous solutions upon the slow heating procedure. Polymer concentration: 1.0 mg/mL; detection angle: 30°.

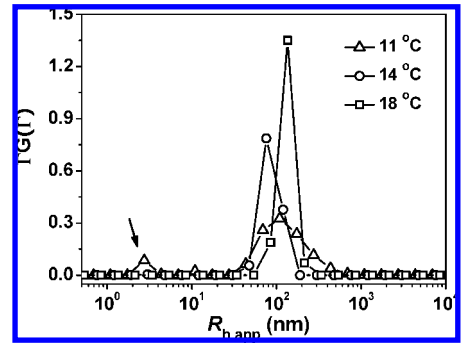

Figure 4. CONTIN analysis of PEG-*b*-P*t*NEA$_{73}$ (**P3**) in 10 mM phosphate buffer (pH 8.4) at different temperatures. Polymer concentration: 1.0 mg/mL; detection angle: 30°.

Thermally Induced Phase Transition. Thermally induced phase transition behaviors of the three block copolymers were first studied using laser light scattering. Figure 3 shows the temperature dependence of the excess scattered intensity of the polymers at a concentration of 1.0 mg/mL, where the polymer solutions were equilibrated at each temperature for 60 min before measurements, i.e., employing the slow heating procedure. It can be seen that the excess scattered intensity of the polymer solutions remained unchanged at temperatures below 13 °C. Upon heating through a critical temperature for each of the polymers, a sharp increase in the scattered intensity, indicating the aggregation of the P*t*NEA block, was detected. We also found that the CAT values were decreased with the increase of P*t*NEA block length. As indicated in the inset in Figure 3, the CATs were 17.5, 14.8, and 13.7 °C for **P1**, **P2**, and **P3**, respectively (Table 1). A similar trend was observed for the block copolymer nanogels of PNIPAM and PEG[27] or the block copolymers of poly(*N*-(2-hydroxypropyl)methacrylamide dilactate) (pHPMAmDL) and PEG.[28]

Figure 4 shows the CONTIN analysis of **P3** sample with varying temperatures at a detection angle of 30°. At temperatures below the CAT (13.7 °C), a bimodal distribution similar to those in Figure 2 was observed. With increasing temperature above the CAT to induce the aggregation (14 °C), the component attributed to the single polymer chains disappeared. The remaining component has a much narrower distribution and a smaller size than the associates at the lower temperatures. However, the size of the aggregates increased with further increasing temperature to 18 °C. The **P1** and **P2** samples exhibited similar results as **P3**, but with the transition temper-

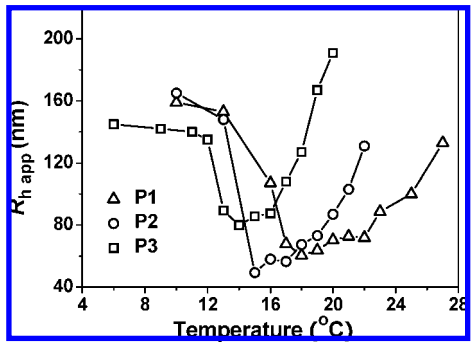

Figure 5. Temperature dependence of the apparent hydrodynamic radii of the polymer aqueous solutions upon the slow heating procedure. Polymer concentration: 1.0 mg/mL, detection angle: 30°.

ature varied differently. Figure 5 compares the temperature dependence of the apparent hydrodynamic radii ($R_{h,app}$) for the three polymers at the same concentration. Below the CATs, only $R_{h,app}$ values of the loose associates were presented. The curves in Figure 5 could be divided into several regions. Using **P3** as an example, at temperatures below 12 °C, $R_{h,app}$ of the loose associate slightly decreased with increasing temperature. This can be mainly attributed to the slight contraction of the polymer chains in the associates because water progressively became a poor solvent for the P*t*NEA block.[29] In the range of ~12−14 °C, $R_{h,app}$ decreased rapidly with increasing temperature; at the same time, a sharp increase in the scattered intensity was observed (inset in Figure 3). In this temperature range, the P*t*NEA block underwent a coil-to-globule transition due to the poor solvent quality, leading to the formation of primary aggregates (also called "particles") with a relatively narrow distribution (Figure 4). Upon further elevating temperature to ~16 °C, the scattered intensity significantly increased but with only a slight increase in $R_{h,app}$, indicating the occurrence of the interparticle association as well as the continued shrinkage of the particles themselves. At temperatures above 16 °C, the interparticle aggregation became dominant, where both the scattered intensity and $R_{h,app}$ drastically increased. With further increasing temperature beyond ~21 °C, macroscopic precipitation was visualized by the eyes, and no valid scattering data were collected. In the case of **P2**, similar results were obtained but without obvious macroscopic precipitation within the tested temperature range. Above their respective CAT, **P2** formed smaller particles than **P3**, which agreed well with the trend for the block copolymers of PNIPAM and PEG.[30]

For the copolymer with the shortest P*t*NEA block, **P1**, two different features were observed. First, the phase transition temperature range of **P1** was broader than that of **P2** or **P3**, which can be attributed to the less magnitude of dehydration of **P1**. Stover et al. reported that PNIPAM with a shorter chain length also showed a broader transition range compared to those with the higher molecular weights.[23a] Second, the scattered intensity of **P1** was much lower than those of the other two polymers. By the combination of the scattered intensity and $R_{h,app}$ values, densities of the formed particles could be evaluated. As shown in Figure 5, the particles formed by **P1** at 27 °C, **P2** at 22 °C, and **P3** at 18 °C were similar in size ($R_{h,app}$ ~130 nm). However, the scattered intensities of **P2** or **P3** were ~4−8 times larger than that of **P1** at the corresponding temperatures, suggesting that **P2** or **P3** had a much stronger aggregation tendency than **P1**. Assuming that the d*n*/d*c* values of the three copolymers are the same, $R_{vv}(q)$ is approximately proportional to the apparent molecular weight ($M_{w,app}$) of the particles (eq 1). The significantly larger scattered intensities demonstrated that the particles formed by **P2** or **P3** above their respective CAT had much larger $M_{w,app}$ than that of **P1**. These results

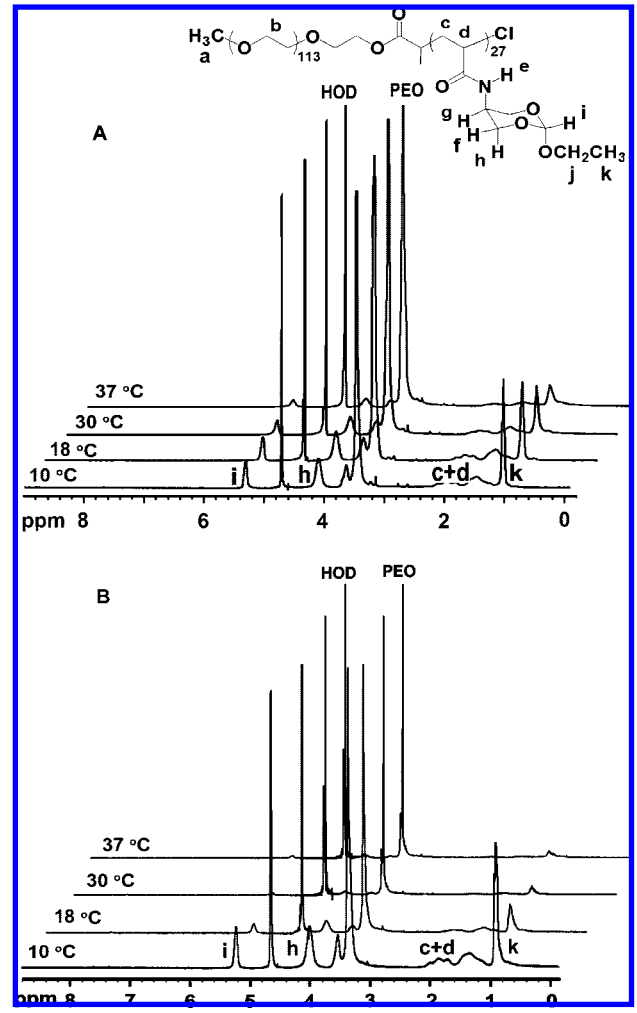

Figure 6. Temperature-dependent ^{1}H NMR spectra of PEG-*b*-P*t*NEA$_{27}$ (**P1**, A) and PEG-*b*-P*t*NEA$_{56}$ (**P2**, B) in the deuterated phosphate buffer (10 mM, pD 8.4). Polymer concentration: 10 mg/mL.

indicate that the particle density of **P1** was much lower than that of **P2** or **P3**, which can be attributed to the less extent of dehydration of **P1** above its CAT as proved by the ^{1}H NMR measurements. Figure 6 shows the temperature-dependent ^{1}H NMR spectra of **P1** and **P2**. It can be seen that both polymers were well solvated below the CATs (10 °C). The proton signals assigned to both P*t*NEA and PEG blocks were observed clearly. For **P2** upon heating through its CAT, the signals of P*t*NEA block were drastically reduced and almost disappeared at the temperatures of 30 °C or higher, while the signals of PEG did not change much. By contrast, although the proton signals of P*t*NEA block of **P1** showed an obvious decrease in intensity, they were clearly observable even at 37 °C, indicating that the thermosensitive P*t*NEA block of **P1** still had some extent of flexibility. A similar phenomenon was also reported for the block copolymers of pHPMAmDL and PEG with different pHPMAmDL lengths.[28]

In general, for systemic drug delivery applications, stable polymeric micelles or nanoparticles with sizes of ~100 nm or less are preferable to achieve a better targeting efficacy.[3,4,31] However, according to the aforementioned results, larger particles (>240 nm in diameter) were obtained by slowly heating the polymer solutions to the temperatures of ~5−10 °C above their respective CAT. In particular for **P3**, obvious macroscopic precipitation was observed at or above ~21 °C. It has been reported that the heating rate is a key factor for tuning the size and morphology of the polymeric micelles or vesicles of the

Table 2. $R_{g,app}$, $R_{h,app}$, and Their Ratios of the Micelles of PEG-*b*-P*t*NEAs[a]

	$R_{g,app}$ (nm)	$R_{h,app}$ (nm)	$R_{g,app}/R_{h,app}$
P1	90.2	73.4	1.23
P2	61.2	61.2	1.00
P3	73.5	68.0	1.08

[a] Determined by DLS ($R_{h,app}$) and SLS ($R_{g,app}$). Polymer concentration: 1.0 mg/mL.

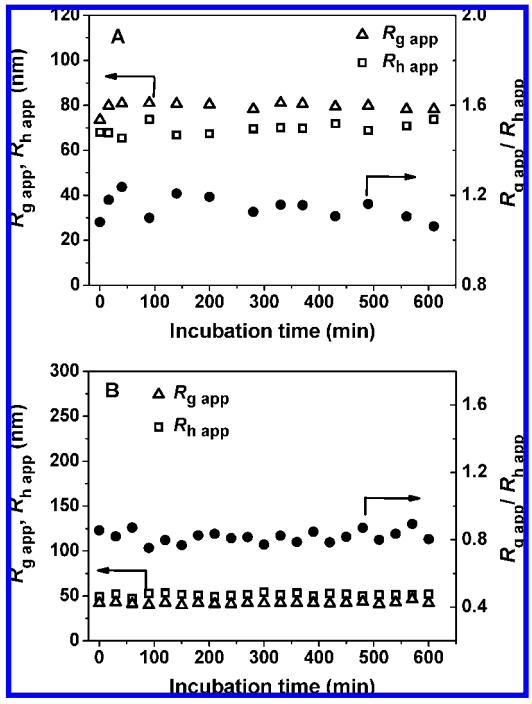

Figure 7. Incubation time-dependent change of $R_{g,app}$ (empty triangle), $R_{h,app}$ (empty square), and $R_{g,app}/R_{h,app}$ (solid circle) of PEG-*b*-P*t*NEA$_{73}$ (**P3**) micelles prepared by the fast heating procedure in 10 mM (A, pH 8.4) and 100 mM (B, pH 7.4) phosphate buffer. 37 °C; polymer concentration: 1.0 mg/mL.

thermosensitive polymers.[28,32] A fast heating procedure is generally beneficial to the formation of smaller particles.[29,33] In order to get micelles or nanoparticles with the expected small sizes that would be stable upon incubation, a fast heating procedure was applied. The polymer solutions in 10 mM phosphate buffer (pH 8.4) below the CATs were quickly heated to 60 °C, left for ~10 min, and then cooled slowly to 37 °C. The solutions for all the three polymers became bluish after reaching equilibrium, but no macroscopic precipitation was observed. A single component with a narrow distribution was detected for all the three polymers (Figure S9). Table 2 summarizes the measured values of $R_{g,app}$, $R_{h,app}$, and the $R_{g,app}/R_{h,app}$ ratio of the particles prepared by the fast heating protocol. These nanoparticles are speculated to have a micelle-like core−shell structure with PEG chains as the shell and P*t*NEA segments as the core, which was supported by their ^{1}H NMR spectra. It is well-known that for typical micelles with a condensed core and a loose shell the values of $R_{g,app}/R_{h,app}$ are generally smaller than 0.775.[32b,34] The larger values of $R_{g,app}/R_{h,app}$ (~1.0−1.2) may indicate that these nanoparticles were loose compound micelles or micellar clusters.[15b,25,35] Clearly, the nanoparticles formulated by the fast heating procedure cannot be achieved by using the slow heating procedure, in that the macroscopic precipitation occurred for **P3** at 37 °C, and the sizes of the particles could be much larger for **P1** and **P2** at the same temperature as predicted by the curves in Figure 5. Figure 7A shows the time-dependent changes of $R_{g,app}$, $R_{h,app}$, and the $R_{g,app}/R_{h,app}$ ratio of the micelles formed from **P3** by the fast heating procedure. It can be seen that the size and morphology of the micelles remained almost unchanged, indicating that these micelles were stable at 37 °C at least for 10 h. The excess scattered intensity also kept constant during the same incubation period (Figure S10).

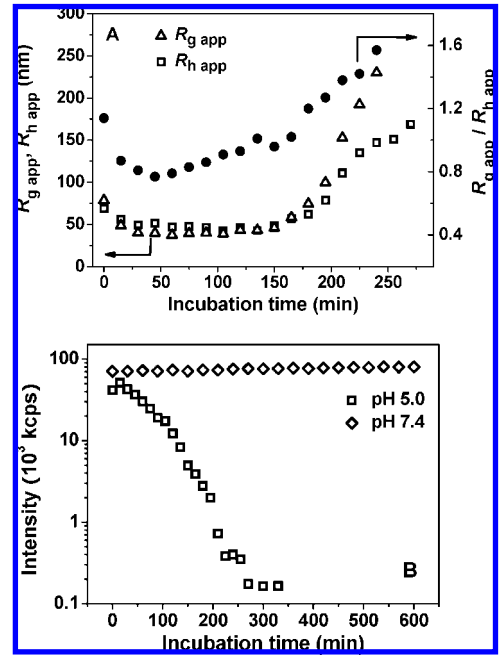

Figure 8. (A) Incubation time-dependent change of $R_{g,app}$ (empty triangle), $R_{h,app}$ (empty square), and $R_{g,app}/R_{h,app}$ (solid circle) of PEG-*b*-P*t*NEA$_{73}$ (**P3**) micelles at at pH 5.0. (B) Incubation time-dependent change of the excess scattered light intensity (30° angle) of **P3** micelles at pH 7.4 and 5.0. The micelles were prepared by the fast heating procedure. Buffer concentration: 100 mM; polymer concentration: 1.0 mg/mL; 37 °C.

Acid-Triggered Destabilization of the Polymeric Micelles. As described previously, the hydrolysis of the pendent cyclic orthoester groups increased the hydrophilicity of the thermoresponsive polymers, and finally the hydrolyzed polymers became completely water-soluble at 37 °C.[17b] In the present work, pH-dependent destabilization behaviors of the polymeric micelles of **P3** were investigated by the light scattering approach. Shown in Figures 7B and 8A are the incubation time-dependent changes in values of $R_{g,app}$, $R_{h,app}$, and their ratio of the micelles at two pHs: 7.4 and 5.0. In order to keep pH values constant during the hydrolysis, the phosphate (pH 7.4) and acetate (pH 5.0) buffers with a concentration of ~100 mM were used for the destabilization experiments. At pH 7.4, a monomodal distribution was observed within the time range of measurements (Figure S11). Moreover, $R_{g,app}$, $R_{h,app}$, and the $R_{g,app}/R_{h,app}$ ratio were almost unchanged, indicating that the micelles were stable. However, compared with those in the 10 mM phosphate buffer (pH 8.4), both the sizes and $R_{g,app}/R_{h,app}$ ratio of the micelles in the 100 mM phosphate buffer at pH 7.4 were significantly reduced, where $R_{g,app}$, $R_{h,app}$, and their ratio decreased from ~80 to ~42 nm, from ~70 to ~52 nm, and from ~1.1 to ~0.8, respectively (Figure 7). This difference can be attributed to the salt effect. $H_2PO_4^-$ (or HPO_4^{2-}) was reported to be the Kosmotropic ion which promotes the dehydration of water-soluble polymers and thus makes the micelles more compact.[36] The decrease in $R_{g,app}/R_{h,app}$ ratio indicated that the salt effect occurred mainly through the core-forming P*t*NEA block even through the hydration degree of PEG chains was also influenced by the salt.[37] The slight increase in the excess scattered intensity at pH 7.4 was probably caused by the enhanced dehydration of PEG chains in the 100 mM buffer, which could reduce its

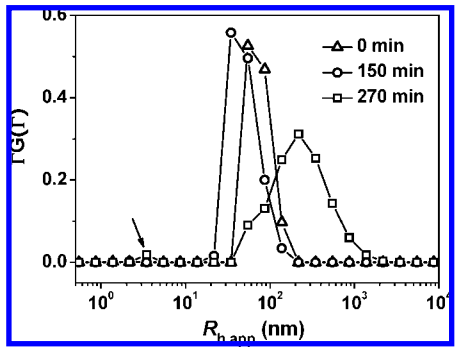

Figure 9. CONTIN analysis of the polymeric micelles at selected time points during the incubation at pH 5.0. The micelles were prepared from PEG-*b*-P*t*NEA$_{73}$ (**P3**) by the fast heating procedure. Polymer concentration: 1.0 mg/mL; detection angle: 30°.

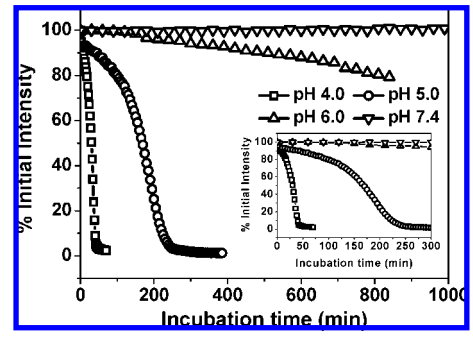

Figure 10. Incubation time-dependent change of the fluorescence intensity at 620 nm of Nile Red in PEG-*b*-P*t*NEA$_{73}$ (**P3**) micelle solutions at different pHs. λ_{ex} = 545 nm; 37 °C; polymer concentration: 1.0 mg/mL; NR concentration: 5.0 × 10^{-6} M.

protection effect and thus induce a little association of the micelles (Figure 8B).

Different behaviors were observed in the acetate buffer (pH 5) (Figure 8). The whole hydrolysis procedure can be divided into four stages. From the beginning to ∼40 min, both the size and $R_{g,app}/R_{h,app}$ ratio were significantly reduced mainly due to the salt-induced chain contraction within the micelles. In the time range of ∼40−135 min, a slight increase in $R_{g,app}$ and a decrease in $R_{h,app}$ occurred, which resulted in an increase in the $R_{g,app}/R_{h,app}$ ratio. In this stage, the excess scattered intensity was drastically declined. These results suggested that the dissociation of the micelles took place in this range, which was accompanied by the swelling of the micellar core due to the partial hydrolysis of the orthoester groups. In the third stage, ∼135−240 min, further hydrolysis of the orthoester groups made the swelling so dominant that $R_{g,app}$, $R_{h,app}$, and their ratio significantly increased. In the same time range, the drastic decrease in the scattered intensity continued, demonstrating the continuous dissociation of the micelles. After the incubation time of ∼240 min, only a little change in the scattered intensity was observed, indicating that the micelles were completely dissociated. Figure 9 shows the size distribution at selected time points during the hydrolysis. The narrowly distributed aggregates maintained its shape before 150 min. In the third stage, where the scattered intensity sharply decreased, the distribution became broad. When the hydrolysis was complete (after 240 min), a bimodal distribution, indicating the coexistence of the single polymer chains and the loose associates, was observed even at a small scattering angle.

pH-Dependent Release of Nile Red. The pH-dependent destabilization of the micelles, which would trigger the release of the hydrophobic payload, was investigated using Nile Red as a model compound. Nile Red is a hydrophobic dye which shows a strong fluorescence peak at ∼620 nm in a hydrophobic microenvironment, but the emission intensity is very weak in aqueous solutions.[9] The micelles of **P3** were first equilibrated with Nile Red in the 10 mM pH 8.4 phosphate buffer at 37 °C, and the pH was adjusted by addition of the concentrated buffers with different pH values. From Figure 10, it is seen that the fluorescence intensity at 620 nm of Nile Red at pH 7.4 remained almost constant in the time range of measurements, indicating that the micelles were stable without obvious dissociation. However, the emission intensities of the samples at lower pHs decreased with the incubation time, suggesting the release of Nile Red from the micelles. The releasing rate of Nile Red drastically increased with the decrease of pH. At pH 5.0, the fluorescence gradually decreased to ∼70% of its original intensity in ∼135 min. A rapid decrease of the intensity occurred within the time range of ∼135−240 min, beyond which only very weak fluorescence was detected. These observations are well consistent with the light scattering results. Before 135 min, the hydrolysis of the orthoester groups was relatively slow because of the hydrophobicity of the micellar core. Thus, only partial dissociation and swelling of the micelles took place in this period, resulting in a slower release of Nile Red. After 135 min, the hydrolysis of the orthoester groups became faster due to the increased hydrophilicity and water content inside the swelled micellar core, which caused the rapid swelling and dissociation of the micelles and the subsequent faster release of Nile Red. Nile Red was also entrapped in the pH-insensitive micelles formed from a styrene-containing block copolymer, PEG_{44}-*b*-PS_{65}, and the fluorescence spectra of the dye-containing micelles in the buffers of pH 7.4 and 5.0 were recorded. Both samples showed similar spectra with strong fluorescence intensities at 620 nm even after being incubated for ∼12 h at 37 °C (data not shown). This result further demonstrated that the acid-triggered release of Nile Red from the micelles of **P3** was attributed to the disruption of the micelles.

Conclusion

We have prepared a novel type of acid-labile thermoresponsive block copolymers with pendent orthoester groups. These polymers are water-soluble at low temperatures but undergo a thermally induced phase transition upon heating through their respective CAT which is dependent on the length of the thermoresponsive block. Acid-sensitive polymeric micelles can be prepared simply by quickly heating the solutions of the block copolymers above their CATs. Hydrophobic compounds such as Nile Red can be encapsulated inside these polymeric micelles, which are stable at pH 7.4 but dissociate to release the payload upon mildly acidic triggering. These block copolymers do not show cytotoxicity (Figure S14), suggesting that the acid-sensitive thermoresponsive micelles formed by the polymers may have great potential as carriers for tumor tissue and/or intracellular drug delivery.

Acknowledgment. This work was financially supported by the National Natural Science Foundation of China (No. 50673004 and 20534010). The authors thank Prof. Zheming Wang for his kind help in X-ray diffraction measurements.

Supporting Information Available: NMR spectra and crystal structures of the monomer, GPC curves, more CONTIN analysis results, emission spectra of Nile Red, MTT assay results, and ^{1}H NMR spectra of **P3** with different hydrolysis times at pD 5.0. This

material is available free of charge via the Internet at http://pubs.acs.org.

References and Notes

(1) (a) Moffitt, M.; Khougaz, K.; Eisenberg, A. *Acc. Chem. Res.* **1996**, *29*, 95–102. (b) Alexandridis, P.; Spontak, R. J. *Curr. Opin. Colloid Interface Sci.* **1999**, *4*, 130–139.

(2) Some typical reviews on polymeric micelles or micellar aggregates: (a) Kataoka, K.; Harada, A.; Nagasaki, Y. *Adv. Drug Delivery Rev.* **2001**, *47*, 113–131. (b) Adams, M. L.; Lavasanifar, A.; Kwon, G. S. *J. Pharm. Sci.* **2003**, *92*, 1343–1355. (c) Gaucher, G.; Dufresne, M.-H.; Sant, V. P.; Kang, N.; Maysinger, D.; Leroux, J.-C. *J. Controlled Release* **2005**, *109*, 169–188. (d) Liggins, R. T.; Burt, H. M. *Adv. Drug Delivery Rev.* **2002**, *54*, 191–202. (e) Kabanov, A. V.; Batrakova, E. V.; Alakhov, V. Y. *J. Controlled Release* **2002**, *82*, 189–212.

(3) (a) Nishiyama, N.; Kataoka, K. *Adv. Polym. Sci.* **2006**, *193*, 67–101. (b) Kwon, G. S.; Suwa, S.; Yokoyama, M.; Okano, T.; Sakurai, Y.; Kataoka, K. *J. Controlled Release* **1994**, *29*, 17–23.

(4) (a) Maeda, H.; Greish, K.; Fang, J. *Adv. Polym. Sci.* **2006**, *193*, 103–121. (b) Matsumura, Y.; Maeda, H. *Cancer Res.* **1986**, *46*, 6387–6392. (c) Seymour, L. W.; Miyamoto, Y.; Maeda, H.; Brereton, M.; Strohalm, J.; Ulbrich, K.; Duncan, R. *Eur. J. Cancer* **1995**, *31A*, 766–770.

(5) (a) Kang, N.; Leroux, J.-C. *Polymer* **2004**, *45*, 8967–8980. (b) Jette, K. K.; Law, D.; Schmitt, E. A.; Kwon, G. S. *Pharm. Res.* **2004**, *21*, 1184–1191. (c) Opanasopit, P.; Yokoyama, M.; Watanabe, M.; Kawano, K.; Maitani, Y.; Okano, T. *Pharm. Res.* **2004**, *21*, 2001–2008.

(6) (a) Rijcken, C. J. F.; Soga, O.; Hennink, W. E.; van Nostrum, C. F. *J. Controlled Release* **2007**, *120*, 131–148. (b) Oh, K. T.; Yin, H. Q.; Lee, E. S.; Bae, Y. H. *J. Mater. Chem.* **2007**, *17*, 3987–4001. (c) Rapoport, N. *Prog. Polym. Sci.* **2007**, *32*, 962–990. (d) Alarcon, C.; Pennadam, S.; Alexander, C. *Chem. Soc. Rev.* **2005**, *34*, 276–285.

(7) (a) Zhang, J. Y.; Zhou, Y. M.; Zhu, Z. Y.; Ge, Z. S.; Liu, S. Y. *Macromolecules* **2008**, *41*, 1444–1454. (b) Shen, X. C.; Zhang, L. Y.; Jiang, X. Q.; Hu, Y.; Guo, J. *Angew. Chem., Int. Ed.* **2007**, *46*, 7104–7107. (c) Cheng, C.; Wei, H.; Shi, B. X.; Cheng, H.; Li, C.; Gu, Z. W.; Cheng, S. X.; Zhang, X. Z.; Zhuo, R. X. *Biomaterials* **2008**, *29*, 497–505. (d) Jiang, J. Q.; Tong, X.; Zhao, Y. *J. Am. Chem. Soc.* **2005**, *123*, 8290–8291. (e) Napoli, A.; Valentini, M.; Tirelli, N.; Muller, M.; Hubbell, J. A. *Nat. Mater.* **2004**, *3*, 183–189.

(8) (a) Martin, T. J.; Prochazka, K.; Munk, P.; Webber, S. E. *Macromolecules* **1996**, *29*, 6071–6073. (b) Giacomelli, C.; Le Men, L.; Borsali, R.; Lai-Kee-Him, J.; Brisson, A.; Armes, S. P.; Lewis, A. L. *Biomacromolecules* **2006**, *7*, 817–828. (c) Lee, E. S.; Oh, K. T.; Kim, D.; Youn, Y. S.; Bae, Y. H. *J. Controlled Release* **2007**, *123*, 19–26. (d) Soppimath, K. S.; Tan, D. C. W.; Yang, Y. Y. *Adv. Mater.* **2005**, *17*, 318–323.

(9) Gillies, E. R.; Jonsson, T. B.; Frechet, J. M. J. *J. Am. Chem. Soc.* **2004**, *126*, 11936–11943.

(10) Gillies, E. R.; Frechet, J. M. J. *Bioconjugate Chem.* **2005**, *16*, 361–368.

(11) Bae, Y.; Fukushima, S.; Harada, A.; Kataoka, K. *Angew. Chem., Int. Ed.* **2003**, *42*, 4640–4643.

(12) Yoo, H. S.; Lee, E. A.; Park, T. G. *J. Controlled Release* **2002**, *82*, 17–27.

(13) (a) Gil, E. S.; Hudson, S. M. *Prog. Polym. Sci.* **2004**, *29*, 1173–1222. (b) Chilkoti, A.; Dreher, M. R.; Meyer, D. E.; Raucher, D. *Adv. Drug Delivery Rev.* **2002**, *54*, 613–630. (c) Jeong, B.; Kim, S. W.; Bae, Y. H. *Adv. Drug Delivery Rev.* **2002**, *54*, 37–51. (d) Schmaljohann, D. *Adv. Drug Delivery Rev.* **2006**, *58*, 1655–1670. (e) Xu, J.; Liu, S. Y. *Soft Matter* **2008**, *4*, 1745–1749.

(14) Kohori, F.; Sakai, K.; Aoyagi, T.; Yokoyama, M.; Yamato, M.; Sakurai, Y.; Okano, T. *Colloids Surf., B* **1999**, *16*, 195–205.

(15) (a) Topp, M. D. C.; Dijkstra, P. J.; Talsma, H.; Feijen, J. *Macromolecules* **1997**, *30*, 8518–8520. (b) Zhang, W. Q.; Shi, L. Q.; Wu, K.; An, Y. L. *Macromolecules* **2005**, *38*, 5743–5747. (c) Yan, J. J.; Ji, W. X.; Chen, E. Q.; Li, Z. C.; Liang, D. H. *Macromolecules* **2008**, *41*, 4908–4913. (d) Qin, S. H.; Geng, Y.; Discher, D. E.; Yang, S. *Adv. Mater.* **2006**, *18*, 2905–2909.

(16) (a) Neradovic, D.; van Nostrum, C. F.; Hennink, W. E. *Macromolecules* **2001**, *34*, 7589–7591. (b) Soga, O.; van Nostrum, C. F.; Fens, M.; Rijcken, C. J. F.; Schiffelers, R. M.; Storm, G.; Hennink, W. E. *J. Controlled Release* **2005**, *103*, 341–353.

(17) (a) Huang, X. N.; Du, F. S.; Ju, R.; Li, Z. C. *Macromol. Rapid Commun.* **2007**, *28*, 597–603. (b) Huang, X. N.; Du, F. S.; Liang, D. H.; Lin, S. S.; Li, Z. C. *Macromolecules* **2008**, *41*, 5433–5440.

(18) (a) Cui, Z. W.; Lee, B. H.; Vernon, B. L. *Biomacromolecules* **2007**, *8*, 1280–1286. (b) Cho, J. Y.; Sohn, Y. S.; Gutowska, A.; Jeong, B. *Macromol. Rapid Commun.* **2004**, *25*, 964–967. (c) Neradovic, D.; Hinrichs, W. L. J.; Kettenes-van den Bosch, J. J.; Hennink, W. E. *Macromol. Rapid Commun.* **1999**, *20*, 577–581.

(19) Stempel, G. H.; Cross, R. P.; Mariella, R. P. *J. Am. Chem. Soc.* **1950**, *72*, 2299–2300.

(20) Bronstein, L. M.; Sidorov, S. N.; Zhirov, V.; Zhirov, D.; Kabachii, Y. A.; Kochev, S. Y.; Valetsky, P. M.; Stein, B.; Kiseleva, O. I.; Polyakov, S. N.; Shtykova, E. V.; Nikulina, E. V.; Svergun, D. I.; Khokhlov, A. R. *J. Phys. Chem. B* **2005**, *109*, 18786–18798.

(21) Ciampolini, M.; Nardi, N. *Inorg. Chem.* **1966**, *5*, 41–44.

(22) (a) Zimm, B. H. *J. Chem. Phys.* **1948**, *16*, 1099–1116. (b) Debye, P. *J. Phys. Colloid Chem.* **1947**, *51*, 18–32.

(23) (a) Xia, Y.; Yin, X. C.; Burke, N. A. D.; Stover, H. D. H. *Macromolecules* **2005**, *38*, 5937–5943. (b) Bontempo, D.; Li, R. C.; Ly, T.; Brubaker, C. E.; Maynard, H. D. *Chem. Commun.* **2005**, 4702–4704. (c) Duan, Q.; Miura, Y.; Narumi, A.; Shen, X. D.; Sato, S.; Satoh, T.; Kakuchi, T. *J. Polym. Sci., Part A: Polym. Chem.* **2006**, *44*, 1117–1124.

(24) (a) Motokawa, R.; Morishita, K.; Koizumi, S.; Nakahira, T.; Annaka, M. *Macromolecules* **2005**, *38*, 5748–5760. (b) Kjoniksen, A.-L.; Nystrom, B.; Tenhu, H. *Colloids Surf., A* **2003**, *228*, 75–83.

(25) Xu, R. L.; Winnik, M. A.; Hallett, F. R.; Riess, G.; Croucher, M. D. *Macromolecules* **1991**, *24*, 87–93.

(26) (a) Wu, G. W.; Chu, B. *Macromolecules* **1994**, *27*, 1766–1773. (b) Yokoyama, M.; Satoh, A.; Sakurai, Y.; Okano, T.; Matsumura, Y.; Kakizoe, T.; Kataoka, K. *J. Controlled Release* **1998**, *55*, 219–229.

(27) Zhu, P. W.; Napper, D. H. *Macromolecules* **1999**, *32*, 2068–2070.

(28) Soga, O.; van Nostrum, C. F.; Ramzi, A.; Visser, T.; Soulimani, F.; Frederik, P. M.; Bomans, P. H. H.; Hennink, W. E. *Langmuir* **2004**, *20*, 9388–9395.

(29) Qiu, X. P.; Wu, C. *Macromolecules* **1997**, *30*, 7921–7926.

(30) Virtanen, J.; Holappa, S.; Lemmetyinen, H.; Tenhu, H. *Macromolecules* **2002**, *35*, 4763–4769.

(31) Alberts, B.; Johnson, A.; Lewis, J.; Raff, M.; Roberts, K.; Walter, P. *Molecular Biology of the Cell*, 4th ed.; Garland Science: New York, 2002; p 746.

(32) (a) Li, Y. T.; Lokitz, B. S.; McCormick, C. L. *Angew. Chem., Int. Ed.* **2006**, *45*, 5792–5795. (b) Zhang, G. Z.; Wu, C. *Adv. Polym. Sci.* **2006**, *195*, 101–176.

(33) (a) Neradovic, D.; Soga, O.; van Nostrum, C. F.; Hennink, W. E. *Biomaterials* **2004**, *25*, 2409–2418. (b) Zhu, P. W.; Napper, D. H. *Langmuir* **2000**, *16*, 8543–8545. (c) Skrabania, K.; Kristen, J.; Laschewsky, A.; Akdemir, O.; Hoth, A.; Lutz, J.-F. *Langmuir* **2007**, *23*, 84–93. (d) Nuopponen, M.; Kalliomaki, K.; Aseyev, V.; Tenhu, H. *Macromolecules* **2008**, *41*, 4881–4886.

(34) Antonietti, M.; Bremser, W.; Schmidt, M. *Macromolecules* **1990**, *23*, 3796–3805.

(35) Yin, H. Q.; Lee, E. S.; Kim, D.; Lee, K. H.; Oh, K. T.; Bae, Y. H. *J. Controlled Release* **2008**, *126*, 130–138.

(36) Zhang, Y. J.; Cremer, P. S. *Curr. Opin. Chem. Biol.* **2006**, *10*, 658–663.

(37) (a) Louai, A.; Sarazin, D.; Pollet, G.; Francoins, J.; Moreaux, F. *Polymer* **1991**, *32*, 713–720. (b) Magnusson, J. P.; Khan, A.; Pasparakis, G.; Saeed, A. O.; Wang, W. X.; Alexander, C. *J. Am. Chem. Soc.* **2008**, *130*, 10852–10853.

MA802138R